A General Method of Flattening Convex Prismatoids into Flat Sheet

Li Chenglei & Zhou Jingqi
Winner of Foo Kean Pew Memorial Prize and
Gold Award of Singapore Mathematical Project Festival 2012

Introduction

Flattening polyhedron has wide-ranging applications in real-life from flattening of shopping bags to astronomy, robotics-making to biomedical appliances involving trestles and stents. The most notable advantage of flattening polyhedron is reducing the space taken up by the original 3D structure and this has attracted considerable attention. By allowing all faces to lie on a single plane, the volume of polyhedron can effectively be reduced to zero. Demaine and Hayes have first shown that all polyhedra have flattened states [1]. However, flattening of polyhedral remains as an open problem in terms of method to find the flattened state of all polyhedral and its continuous folding motion. While Demaine and O'Rourke have proposed the idea of disk-packing from 2D fold-and-cut problem, the disk-packing method is limited to polyhedra which are homeomorphic to a disk or a sphere [2]. In particular, Bern and Hayes have proven that flattened states exist for an orientable piecewise-linear (PL) 2-manifold [3]. However, disk-packing method requires that the polyhedra are extended to 4D in the folding process [2]. In this paper, we propose a method to flatten all convex prismatoids. Our proposed method can also be used to flatten convex polyhedra as all convex polyhedra can be sliced into several sections of convex prismatoids. We present the algorithm for drawing the "expanded view" from the projection and height of a convex prismatoid, and introduce the general algorithm for “flattening”. We also illustrate the capabilities of our algorithm via several convex polyhedral test examples.

Convex Prismatoid

The convex prismatoids discussed in this paper are described by projection and height.

The roof plane and the base plane of a convex prismatoid are defined as the two parallel planes which all vertices of the prismatoid are located at.

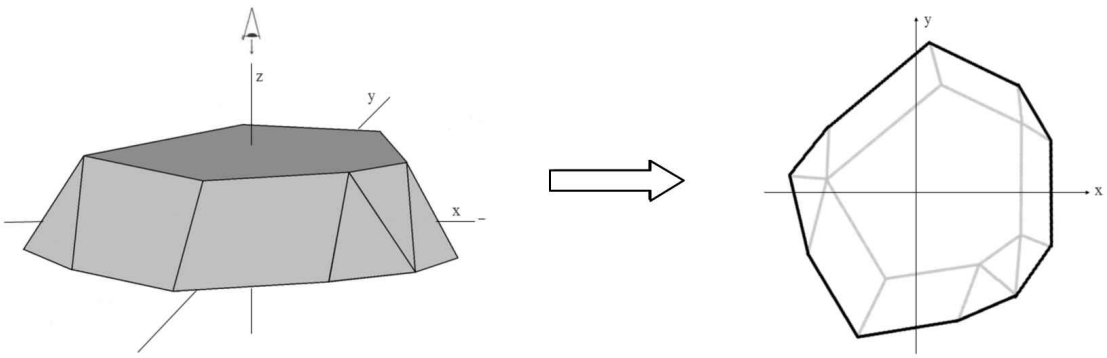

Fig 1: Projection of Prismatoid

A projection of the convex prismatoid (Fig 1) is defined as an aerial view of the prismatoid, drawn on the base plane. This is the same as tracing the shadows of the prismatoid edges cast onto the base plane by vertical light rays. A projection of any prismatoid part is drawn in a similar fashion.

Notation (See Fig 2a) The height of the target prismatoid is denoted by h, the length of the segment of lateral face is denoted by s_i, the altitude of a lateral face is denoted by t, and the projection of t is denoted by l.

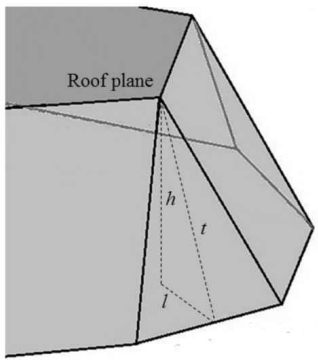

(a) Length h, t and l

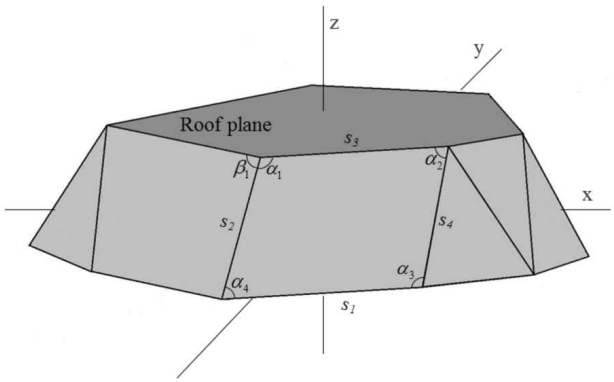

(b) α_i and s_i (quadrilateral lateral face)

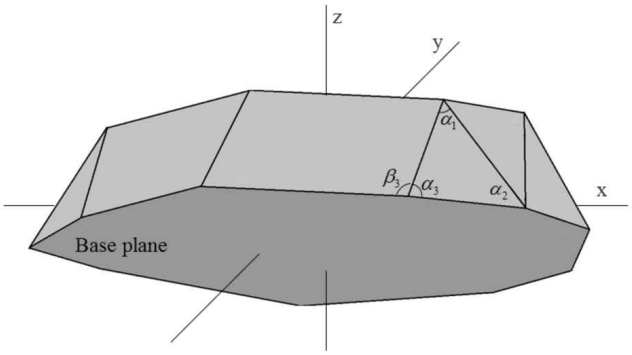

(c) α_i and s_i (triangular lateral face)

Fig 2: Denotation on prismatoid

Lateral faces of convex prismatoids are either triangles or quadrilaterals. On each quadrilateral lateral face (Fig 2b), we denote the angles in clockwise direction as α_1, α_2, α_3 and α_4, with angles α_1 and α_2 adjacent to the roof plane; angles α_3 and α_4, adjacent to the base plane. Angles α_1 and α_4 are supplementary angles; angles α_2 and α_3 are supplementary angles. Then we denote the four adjacent angles of these four angles as β_1, β_2, β_3 and β_4 respectively. Each pair of α and β shares a vertex which is also shared by a third angle located either on roof plane or base plane. This third angle is denoted by γ. We denote the four sides opposite to the four angles correspondingly as s_1, s_2, s_3 and s_4.

On each triangular lateral face (Fig 2c), among its three vertices, one of them lies in one plane. We call this point the apex of the triangle. We denote the apex angle as α_1, and the other two angles as α_2 and α_3. Then denote the two adjacent angles of α_2 and α_3 on adjacent

lateral faces as β_2 and β_3 respectively. Also, each pair of α and β shares a vertex which is also shared by a third angle located on the base plane. This third angle is denoted by γ. We denote the three sides opposite to the three angles correspondingly as s_1, s_2 and s_3.

Method Overview

(A) Projection of Prismatoid

Lemma 1 On any prismatoid, the length of any segment whose end points are on either the roof plane or the base plane can be obtained if the height of the prismatoid and its projection are known.

Proof: For all prismatoids, the roof plane is parallel to the base plane. Upon projection, any segments that are parallel to either plane preserve their lengths.

On the other hand, for other segments, such as $\overline{ab}$, which are not parallel to either plane, their lengths are reduced to $\overline{a'b'}$ upon projection. By visualising the triangle formed by segments $\overline{ab}$, $\overline{a'b'}$ and the height of the prismatoid, h, length of $\overline{ab}$ can be obtained by Pythagoras's Theorem as long as the projection and height of the prismatoid are given.

Similarly, we have the relation $t^2 = l^2 + h^2$ for t, l and h.

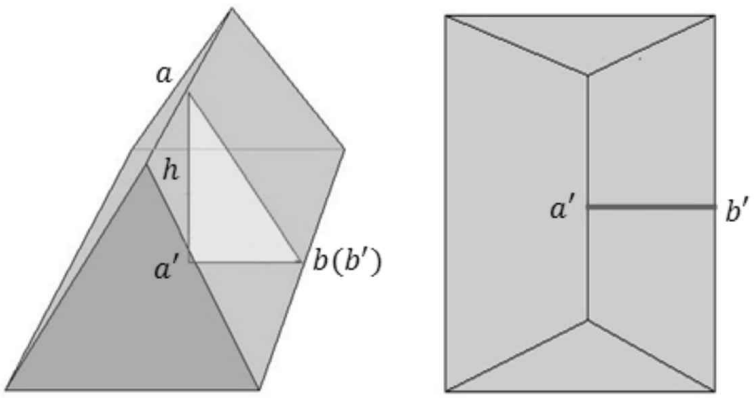

(a) Visualisation of the triangle formed by ab, $a'b'$ and h

(b) Projection of segment ab

Fig 3: Proof of Lemma 1

(B) General Algorithm

Our main approach is to tuck the lateral faces into spaces between the roof plane and the base plane. Hence, the layout of the resultant 2D flattened state is congruent to the projection of the 3D polyhedron.

Upon tucking lateral faces into spaces between roof plane and base plane, a "five valley line" crease pattern will emerge on each lateral face. One "middle valley line" is parallel to the roof plane and the base plane, while another four valley lines extend from four vertices of the lateral face.

Since the lateral faces of prismatoids are either triangular lateral faces or quadrilateral lateral faces, in the general algorithm, we consider all possible combinations of lateral faces, and deal with each combination separately.

General Algorithm

1. Find the positions of the middle valley lines for each lateral face.
2. Check all the lateral faces. Classify them into three cases.
    Case I: Quadrilateral lateral face
        A. Adjacent to quadrilateral lateral face
        B. Adjacent to triangular lateral face whose apex is located on the roof plane
        C. Adjacent to triangular lateral face whose apex is located on the base plane
    Case II: Triangular lateral face whose apex is located on the roof plane
        A. Adjacent to quadrilateral lateral face
        B. Adjacent to triangular lateral face whose apex is located on the roof plane
        C. Adjacent to triangular lateral face whose apex is located on the base plane
    Case III: Triangular lateral face whose apex is located on the base plane
3. Implement methods of drawing valley lines for each case.
4. Add mountain lines accordingly.

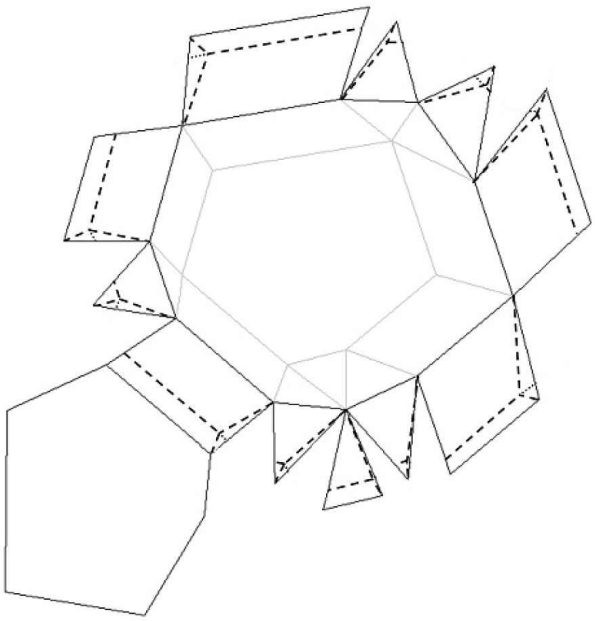

Fig 4: Resultant crease pattern
(dotted lines, dashed lines represent mountain, valley respectively)

Main result

(A) Algorithm for drawing middle valley lines

Proposition 2 Let x_1 denotes the distance from the roof segment to the "middle valley line"; x_2 denotes the distance from the base segment to the "middle valley line". Then

$$x_1 = \frac{t-l}{2} \quad \text{and} \quad x_2 = \frac{t+l}{2}.$$

Proof: Since the layout of the resultant pattern upon flattening is the same as the layout of the projection of the prismatoid, the "middle valley line" on each lateral face is parallel to the roof plane and the base plane.

The "middle valley line" divides the lateral face into two portions which overlap in the flattened state (shown in Fig 5b). The heights of these two portions are x_1 and x_2 respectively.

From $x_1 + x_2 = t$ and $x_2 - x_1 = l$, we obtain $x_1 = \dfrac{t-l}{2}$ and $x_2 = \dfrac{t+l}{2}$.

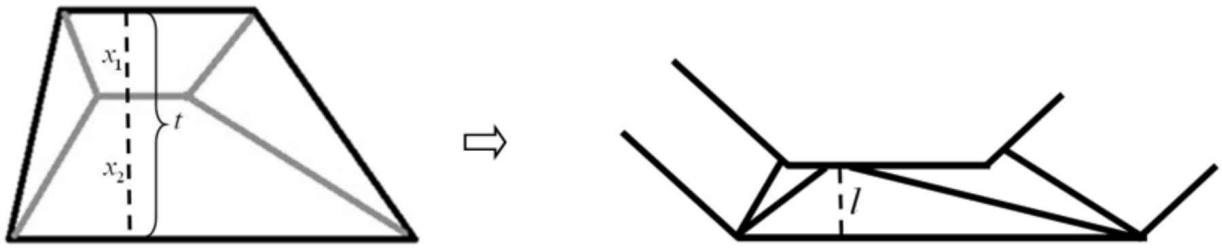

(a) lateral face before flattening (b) flattened state of lateral face

Fig 5: Overlap of the two portions (with height x_1 and x_2) of lateral face upon folding

We denote the dihedral angle between a lateral face and the base plane as δ (Fig 6). Then, $l = t \cdot \cos\delta$, $x_1 = \dfrac{t(1-\cos\delta)}{2}$ and $x_2 = \dfrac{t(1+\cos\delta)}{2}$.

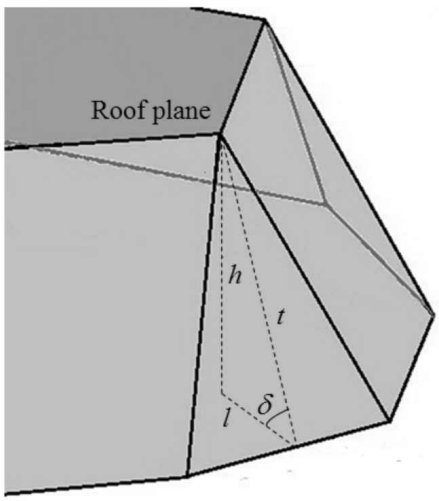

Fig 6: The dihedral angle δ

General Algorithm Step 1

Case I. Quadrilateral lateral face

a. Start with the expanded view. The grey lines which represent the projections are for construction.

b. Mirror copy the projection along the base segment of the lateral face.

c. Find the perpendicular bisector of the corresponding end points as shown.

d. Erase the grey lines constructed in step 2.

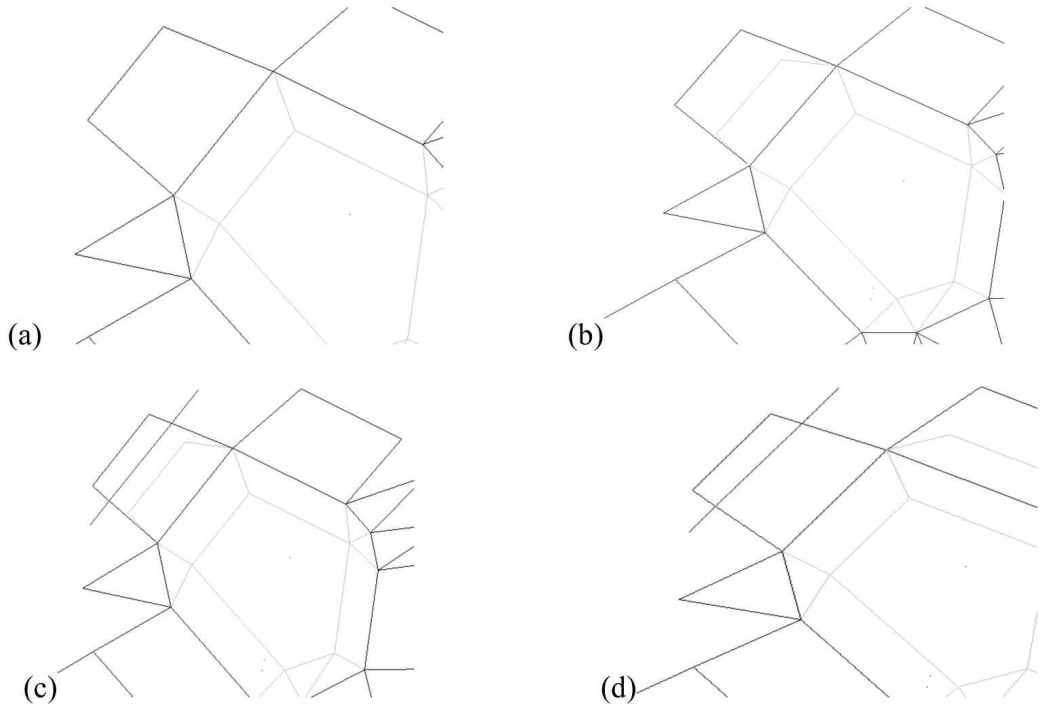

Fig 7: General Algorithm Step 1 for Case I

Case II. Triangular lateral face whose apex is located on the roof plane

a. Start with the expanded view. The grey lines which represent the projections are for construction.

b. Mirror copy the projection along the base segment of lateral face.

c. Find the perpendicular bisector of the corresponding end points as shown.

d. Erase the grey lines constructed in step 2.

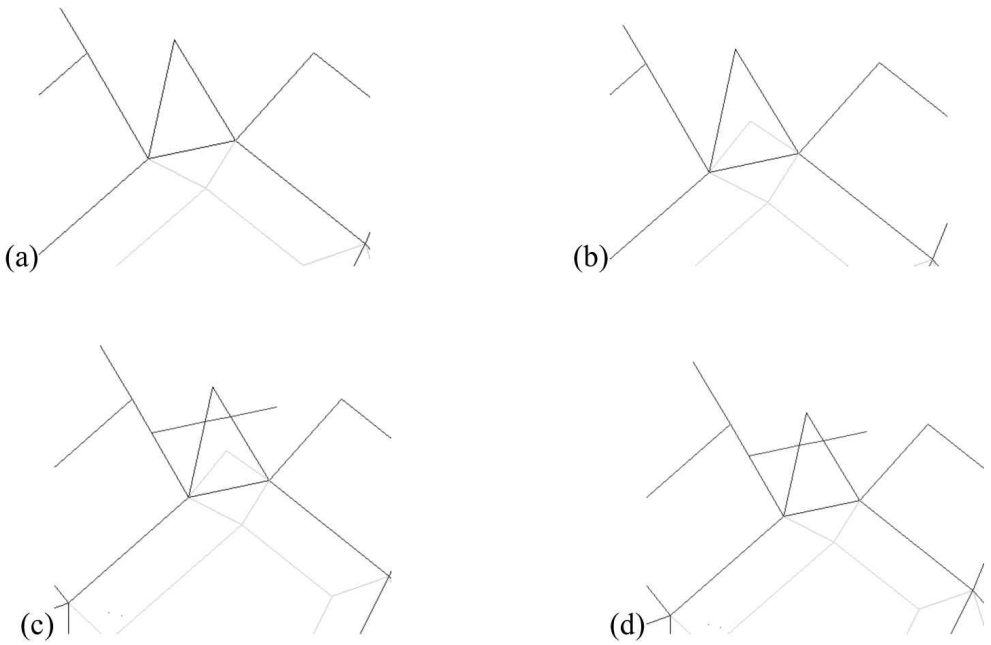

Fig 8: General Algorithm Step 1 for Case II

Case III. Triangular lateral face whose apex is located on the base plane

a. Start with the expanded view. The grey lines which represent the projections are for construction.

b. Construct the height of projection, and the perpendicular of the height passing through the apex of the triangular lateral face.

c. Mirror copy the projection along the perpendicular constructed previously.

d. Find the perpendicular bisector of the corresponding end points as shown.

e. Erase the grey lines constructed in step 2 and 3.

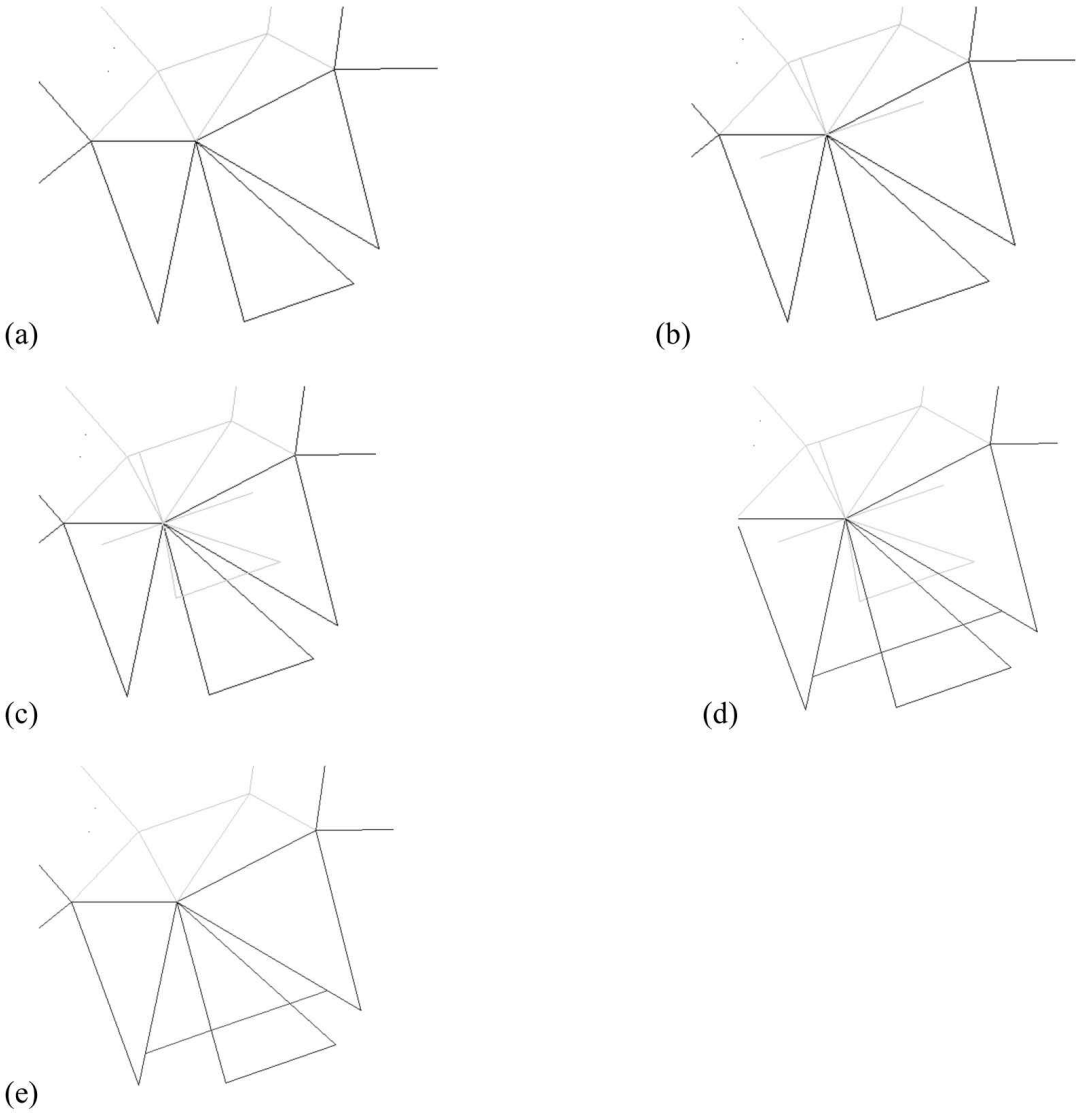

Fig 9: General Algorithm Step 1 for Case III

(B) Algorithm for drawing another four valley lines

Lemma 3 For any vertex surrounded by three angles on three faces, we denote the three angles as α, β and γ. Put the face corresponding to angle γ as bottom and flatten the other two faces, a spare part corresponding to angle θ is obtained, and $\theta = \dfrac{\alpha + \beta - \gamma}{2}$.

Proof: According to Kawasaki's Theorem, the crease pattern may be folded flat if and only if the alternating sum and difference of the angles adds to zero.

In our case, $\alpha - \frac{\alpha+\beta-\gamma}{2} + \left(\beta - \frac{\alpha+\beta-\gamma}{2}\right) - \gamma = 0$, which agrees with Kawasaki's Theorem.

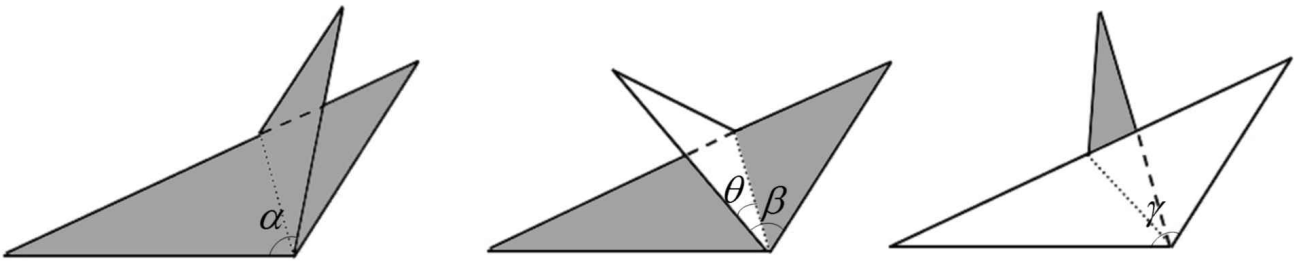

Fig 10: Proof of Lemma 3

Case I (Quadrilateral lateral face)

Valley line pattern

Since the position of the middle valley line has been found in previous step, any one valley line emanating from one of the two vertices from one side is able to indicate the position of the other valley line.

For **Case I A** (adjacent to quadrilateral lateral face), each of its two vertices on one side is surrounded by three faces, which fulfills the condition of Lemma 3. The two valley lines emanating from the two vertices can be found.

Algorithm

a. Continue from general algorithm step 1.

b. By applying Lemma 3, draw valley lines emanating from vertices labelled in the circles.

c. Erase extra portion of the middle valley line.

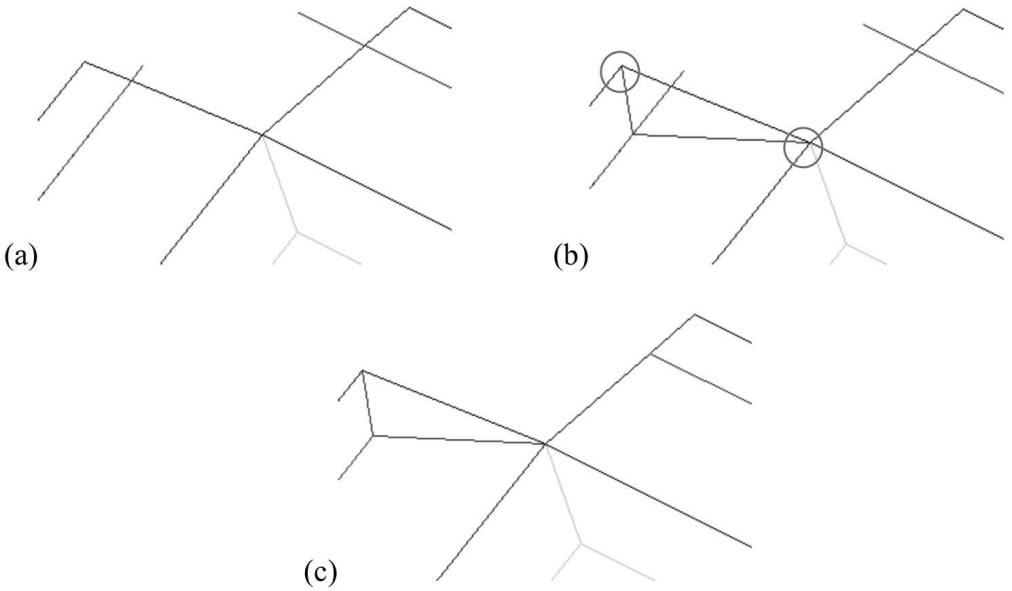

Fig 11: General Algorithm Step 2 for Case I A

For **Case I B** (adjacent to triangular lateral face whose apex is located on the roof plane), the vertex located on the base plane is surrounded by three faces while the vertex located on the roof plane is surrounded by more than three faces.

Although the valley line pattern can be found without knowing the angle a, angle a can be calculated as shown in proposition 4 below.

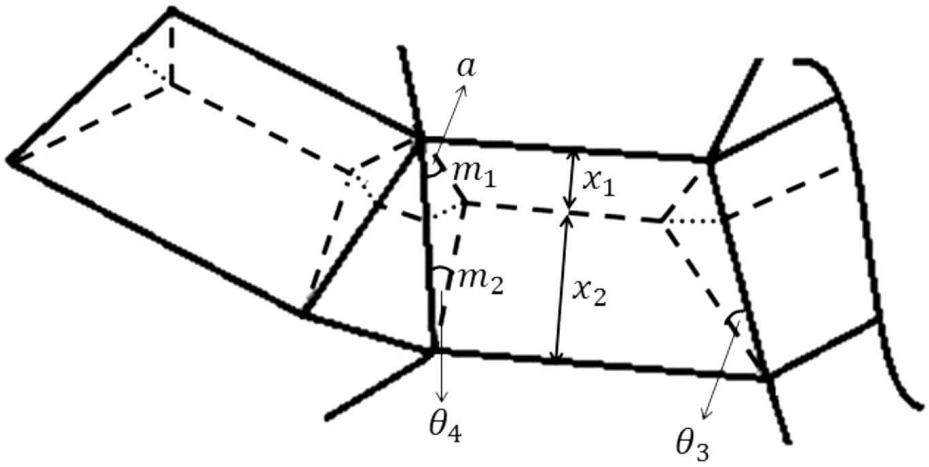

Fig 12: Pattern of quadrilateral lateral face adjacent to triangular lateral face

Proposition 4 The angle a is given by

$$a = \tan^{-1}\left(\frac{x_2 \cdot \sin(\theta_4)\sin(\alpha_1)}{x_1 \cdot \sin(\alpha_4 - \theta_4) + x_2 \cdot \sin(\theta_4)\cos(\alpha_1)}\right).$$

Proof: With the notation given in Fig 12, we have

$$m_2 = \frac{x_1}{\sin(\alpha_1 - a)} \text{ and } m_1 = \frac{x_2}{\sin(\alpha_4 - \theta_4)}.$$

Applying sine rule to the highlighted triangle, we have $\frac{m_1}{\sin a} = \frac{m_2}{\sin(\theta_4)}$.

Hence,

$$\frac{x_2}{\sin(\alpha_4 - \theta_4)\sin a} = \frac{x_1}{\sin(\alpha_1 - a)\sin(\theta_4)}.$$

On simplifying, we get

$$\tan a = \frac{x_2 \cdot \sin(\theta_4)\sin(\alpha_1)}{x_1 \cdot \sin(\alpha_4 - \theta_4) + x_2 \cdot \sin(\theta_4)\cos(\alpha_1)}.$$

Therefore,

$$a = \tan^{-1}\left(\frac{x_2 \cdot \sin(\theta_4)\sin(\alpha_1)}{x_1 \cdot \sin(\alpha_4 - \theta_4) + x_2 \cdot \sin(\theta_4)\cos(\alpha_1)}\right).$$

Algorithm

a. Continue from general algorithm step 1.

b. By applying Lemma 3, draw the valley line emanating from vertices labelled in the circle.

c. Construct the other valley line by connecting intersection point formed in step 2 and vertex labelled in the circle. Erase extra portion of the middle valley line.

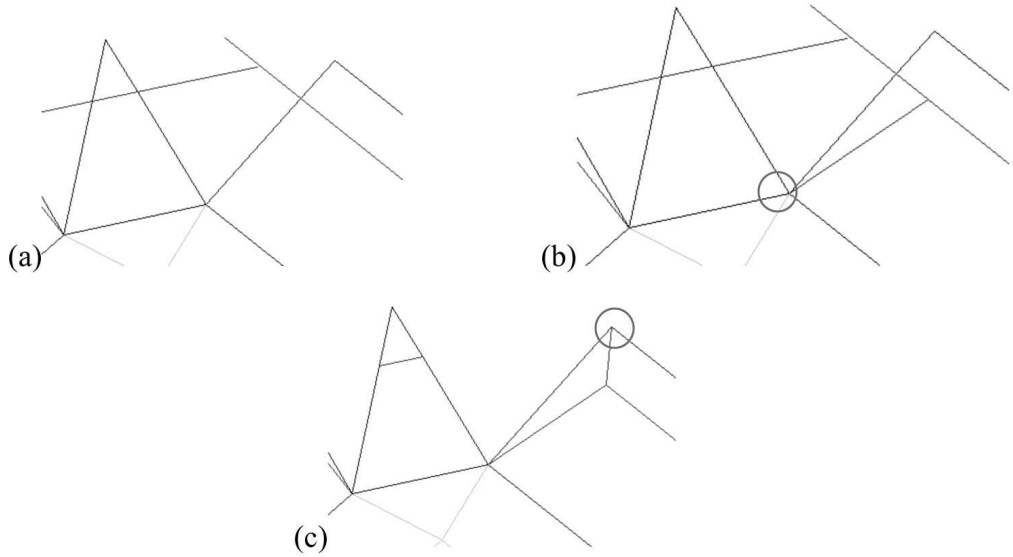

Fig 13: General Algorithm Step 2 for Case I B

For **Case I C** (adjacent to triangular lateral face whose apex locates on the base plane), we may switch the roof plane and the base plane, and the situation becomes Case I B mentioned above.

Limitations and solutions

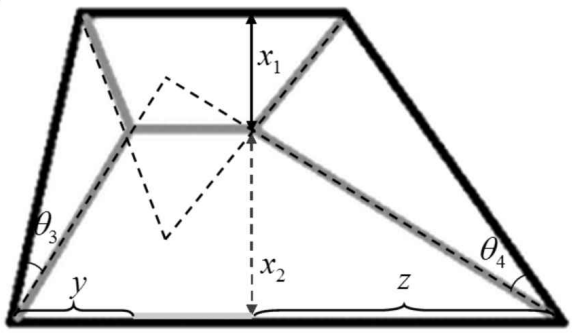

Fig 14: Notation on the quadrilateral lateral face

Proposition 5 The length of the middle valley line is given by

$$s-\frac{t\left(\cos\delta+1\right)\sin\left(\alpha_3-\theta_3+\alpha_4-\theta_4\right)}{2\sin\left(\alpha_3-\theta_3\right)\sin\left(\alpha_4-\theta_4\right)}.$$

Proof: In General Algorithm step 1, we have obtained the middle valley line on all lateral faces. Translate this middle valley line to the lower edge of the lateral face, the length of this line can

then be expressed as $s - y - z$. Segments y and z are shown in Fig14.

By applying trigonometry identity to the two right-angled triangles with catheti y and x_2, and with catheti z and x_2, we get

$$y = \frac{x_2}{\tan(\alpha_2 - \theta_2)} \quad \text{and} \quad z = \frac{x_2}{\tan(\alpha_2 - \theta_3)}.$$

Substituting $x_2 = \frac{t(\cos\delta + 1)}{2}$ (from Proposition 2) into y and z, the length of the middle valley line is given by

$$s - \frac{x_2}{\tan(\alpha_4 - \theta_4)} - \frac{x_2}{\tan(\alpha_3 - \theta_3)}$$

$$= s - \frac{t(\cos\delta + 1)}{2\tan(\alpha_4 - \theta_4)} - \frac{t(\cos\delta + 1)}{2\tan(\alpha_3 - \theta_3)}$$

$$= s - \frac{t(\cos\delta + 1)\sin(\alpha_3 - \theta_3 + \alpha_4 - \theta_4)}{2\sin(\alpha_3 - \theta_3)\sin(\alpha_4 - \theta_4)}.$$

In the real situation, there are three possible valley line patterns in total, as shown in Fig 15.

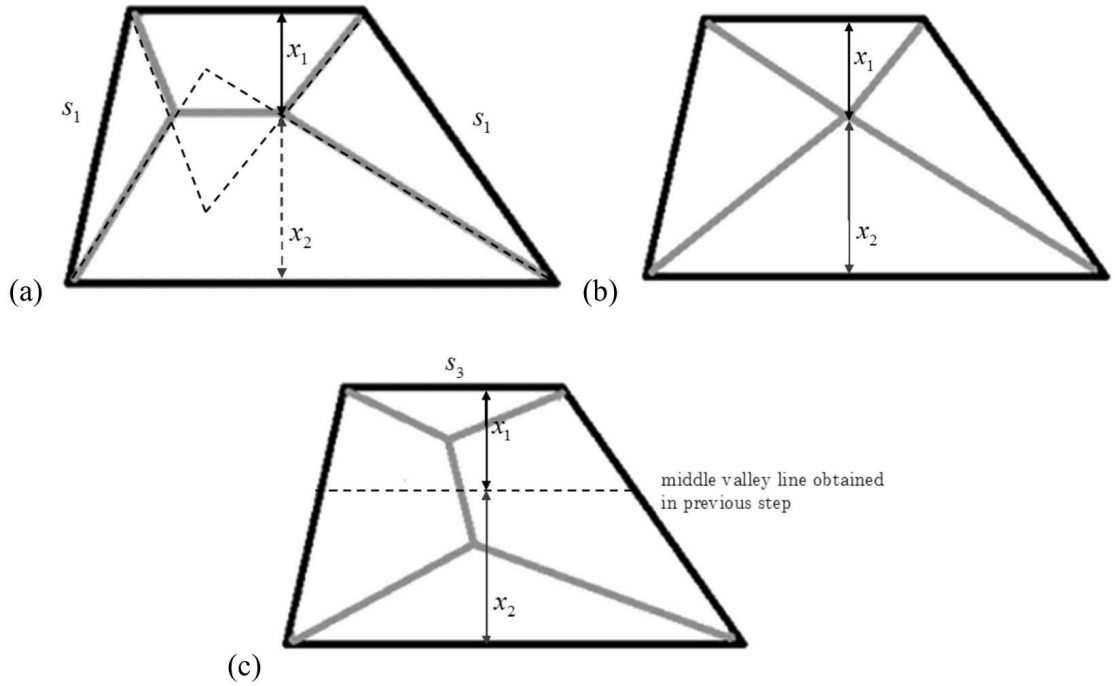

Fig 15: Three possible valley line patterns on a quadrilateral face

In the first pattern shown in Fig 15(a), the two end points of the middle valley line are intersection point of two valley lines extending from vertices on s_1, and intersection point of two valley lines extending from vertices on s_2. The length of the middle valley line is positive.

In the second pattern shown in Fig 15(b), four valley lines extending from four vertices

intersect at a common point. The length of the middle valley line is zero.

In the third pattern shown in Fig 15(c), the two valley lines extending from vertices on s_3 intersect before intersecting with the middle valley line. The length of the middle valley line is negative (shown in dashed line). In this case, limitation exists.

Since the angle θ is determined by the vertex angles of the two planes and the lateral faces, the nature of limitation is that the height of the lateral face t, being greater than its limiting value.

Proposition 6 The maximum height of the lateral face t which does not lead to limitation is:

$$t = \frac{2s \cdot \sin(\alpha_3 - \theta_3)\sin(\alpha_4 - \theta_4)}{(\cos\delta + 1)\sin(\alpha_3 - \theta_3 + \alpha_4 - \theta_4)}.$$

Proof. The maximum t exists when four valley lines emanating from four vertices intersect at a common point, indicating that the length of the middle valley line is 0. By Proposition 5, we have

$$s - \frac{t(\cos\delta + 1)\sin(\alpha_3 - \theta_3 + \alpha_4 - \theta_4)}{2\sin(\alpha_3 - \theta_3)\sin(\alpha_4 - \theta_4)} = 0.$$

Simplifying, we get

$$t = \frac{2s \cdot \sin(\alpha_3 - \theta_3)\sin(\alpha_4 - \theta_4)}{(\cos\delta + 1)\sin(\alpha_3 - \theta_3 + \alpha_4 - \theta_4)}.$$

In order to compute the limitation, the height of the lateral face has to be reduced by dividing the whole prismatoid into several sections.

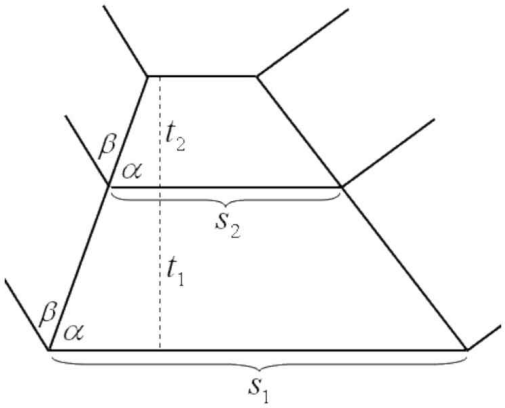

Fig 16: Slicing of prismatoid into sections

Theorem 7 If $\sum_{n=1}^{k-1} t_n < t \le \sum_{n=1}^{k} t_n$, then the least number of sections required is k, where

$$t_{n+1} = t_n\left(1 - \frac{2\sin(\alpha_3 + \alpha_4)\sin(\alpha_3 - \theta_3)\sin(\alpha_4 - \theta_4)}{(\cos\delta + 1)\sin(\alpha_3)\sin(\alpha_4)\sin(\alpha_3 - \theta_3 + \alpha_4 - \theta_4)}\right).$$

Proof. We denote the maximum height of the n^{th} section from the bottom edge up as t_n, and its corresponding (created) bottom edge as s_n. From Proposition 6, the maximum height is

given by $t_n = \dfrac{2s_n \cdot \sin(\alpha_3 - \theta_3)\sin(\alpha_4 - \theta_4)}{(\cos\delta + 1)\sin(\alpha_3 - \theta_3 + \alpha_4 - \theta_4)}$.

Rewriting the equation, we get $s_n = \dfrac{t_n(\cos\delta + 1)\sin(\alpha_3 - \theta_3 + \alpha_4 - \theta_4)}{2\sin(\alpha_3 - \theta_3)\sin(\alpha_4 - \theta_4)}$. (*)

In view of Fig 16, upon slicing, angles α, β, γ remain unchanged. Together with Proposition 6, this implies that t_1 is directly proportional to s_1. The bottom edge of the next section s_2 is then dependent on t_1 and s_1. Thus, given the bottom edge of the prismatoid s_1, the bottom edges and height of each section can then be found.

By trigonometry, $s_{n+1} = s_n - \dfrac{t_n}{\tan(\alpha_3)} - \dfrac{t_n}{\tan(\alpha_4)}$.

Substitute (*) into the above, we have

$$\frac{t_{n+1}(\cos\delta + 1)\sin(\alpha_3 - \theta_3 + \alpha_4 - \theta_4)}{2\sin(\alpha_3 - \theta_3)\sin(\alpha_4 - \theta_4)} = \frac{t_n(\cos\delta + 1)\sin(\alpha_3 - \theta_3 + \alpha_4 - \theta_4)}{2\sin(\alpha_3 - \theta_3)\sin(\alpha_4 - \theta_4)} - \frac{t_n \cdot \sin(\alpha_3 + \alpha_4)}{\sin(\alpha_3)\sin(\alpha_4)}$$

$$t_{n+1} = t_n - \frac{2t_n \cdot \sin(\alpha_3 + \alpha_4)\sin(\alpha_3 - \theta_3)\sin(\alpha_4 - \theta_4)}{(\cos\delta + 1)\sin(\alpha_3)\sin(\alpha_4)\sin(\alpha_3 - \theta_3 + \alpha_4 - \theta_4)}$$

$$t_{n+1} = t_n\left(1 - \frac{2\sin(\alpha_3 + \alpha_4)\sin(\alpha_3 - \theta_3)\sin(\alpha_4 - \theta_4)}{(\cos\delta + 1)\sin(\alpha_3)\sin(\alpha_4)\sin(\alpha_3 - \theta_3 + \alpha_4 - \theta_4)}\right).$$

An expanded view of triangular prism is shown below (Fig 17) as an example of the solution to the limitation. By creating seven parallel mountain lines on each of its lateral faces, it is divided into eight sections. Flattening each section separately will flatten the entire prismatoid.

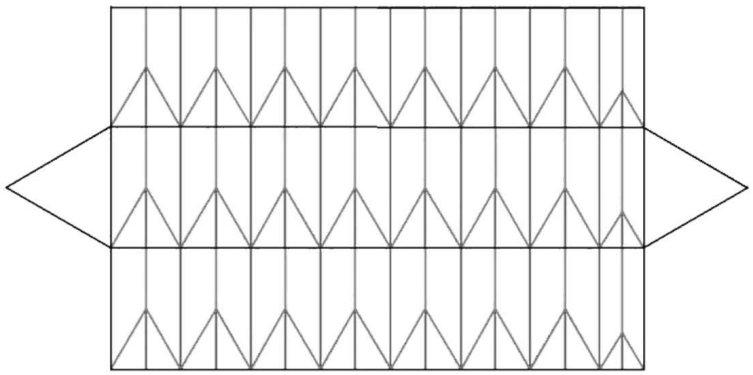

Fig 17: Example of the solution to the limitation

Case II (Triangular lateral face whose apex is located on the roof plane)

For **Case II A**, the two valley lines emanating from two vertices shared by the two lateral faces (triangular and quadrilateral lateral faces) are described by Lemma 3. The situation is similar to Case I B.

When considering real-life application, the more ideal flattened state is that the spare part overlaps with the quadrilateral face. So both valley lines are drawn on quadrilateral lateral face, and no other valley line is required on the triangular lateral face besides the previous middle valley line.

For **Case II B**, the sole valley line emanating from the vertex shared by the two lateral faces (two triangular lateral faces) on the base plane fulfills the condition of Lemma 3.

The other valley line can be obtained when the position of the middle valley line is known in general algorithm step 1.

Algorithm:

a. Continue from general algorithm step 1.

b. By applying Lemma 3, draw the valley line emanating from vertices labelled in the circle.

c. Construct the other valley line by connecting intersection point formed in step 2 and vertex labelled in the circle. Erase extra portion of the middle valley line.

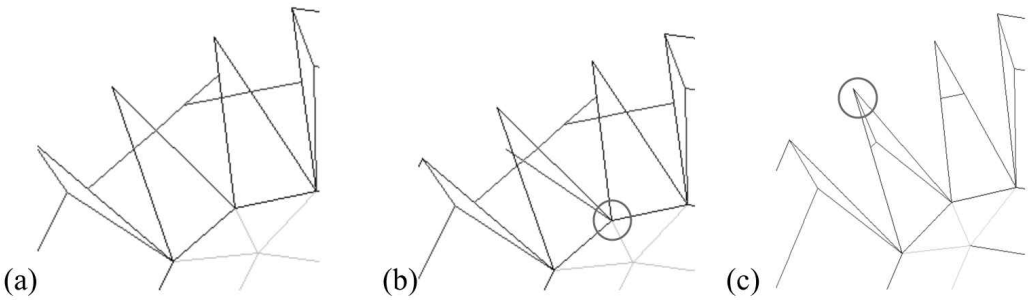

Fig 18: General Algorithm Step 2 for Case II B

For **Case II C**, a new concept is introduced because neither of the two vertices shared by the two triangular lateral faces (one with apex located on the roof plane and the other one with apex located on the base plane) is surrounded by three faces only.

Lemma 8 Similar to Lemma 3, we know that

$$\sum_{n=1}^{k}\theta_n \text{ (sum of angles of all spare parts)} = \frac{1}{2}\left(\sum_{n=1}^{k}\alpha - \gamma\right)$$

where α runs through the vertex angles of the lateral faces surrounding the common vertex, and γ is the angle on the roof plane.

Thus, if the angles of the spare parts on the other faces are known, the spare part between the two triangular lateral faces in this case can be obtained.

So, we may deal with this special case after finding the valley line pattern of the other cases mentioned previously. After obtaining the angle of the spare part between the two triangular lateral faces, with the knowledge of middle valley line obtained in general algorithm step 1, the third valley line emanating from the vertex located on the base plane is known as well.

Algorithm:

a. Continue from general algorithm step 1.

b. By applying Lemma 8, draw the valley line emanating from vertices labelled in the circle.

c. Construct the other valley line by connecting the intersection point formed in step 2 and vertex labelled in the circle. Erase extra portion of the middle valley line.

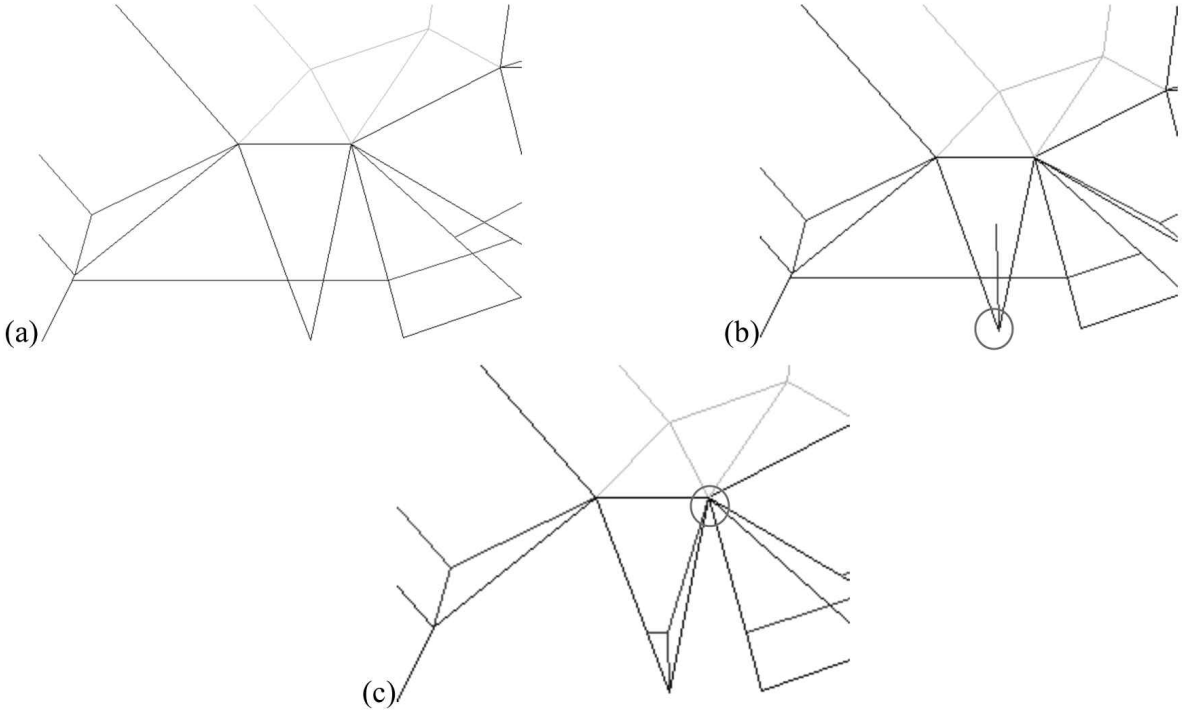

Fig 19: General Algorithm Step 2 for Case II C

Case III (Triangular lateral face whose apex is located on the base plane)

We may switch the roof plane and the base plane, and use the same technique in Case II to deal with this case.

(C) Drawing the mountain lines

Mountain lines appear naturally when we fold along the valley line patterns. To draw them, simply connect all middle valley lines on all lateral faces.

Implementation and results

We have implemented our proposed algorithms manually to fold convex prismatoids given in examples 1- 6 (Figs. 20 - 25). These examples are specifically chosen for their varied structures to test the correctness and capabilities of the algorithm. Projection (a) of each example is drawn manually. We have drawn the expanded view with crease pattern (b) for flattening by following our proposed algorithms. The 3D structure (c) as well as the flattened state (d) of the convex prismatoid are then shown.

Example 1 (Fig 20) is a rotationally symmetric frustum. Its layout of roof plane and layout of base plane are similar.

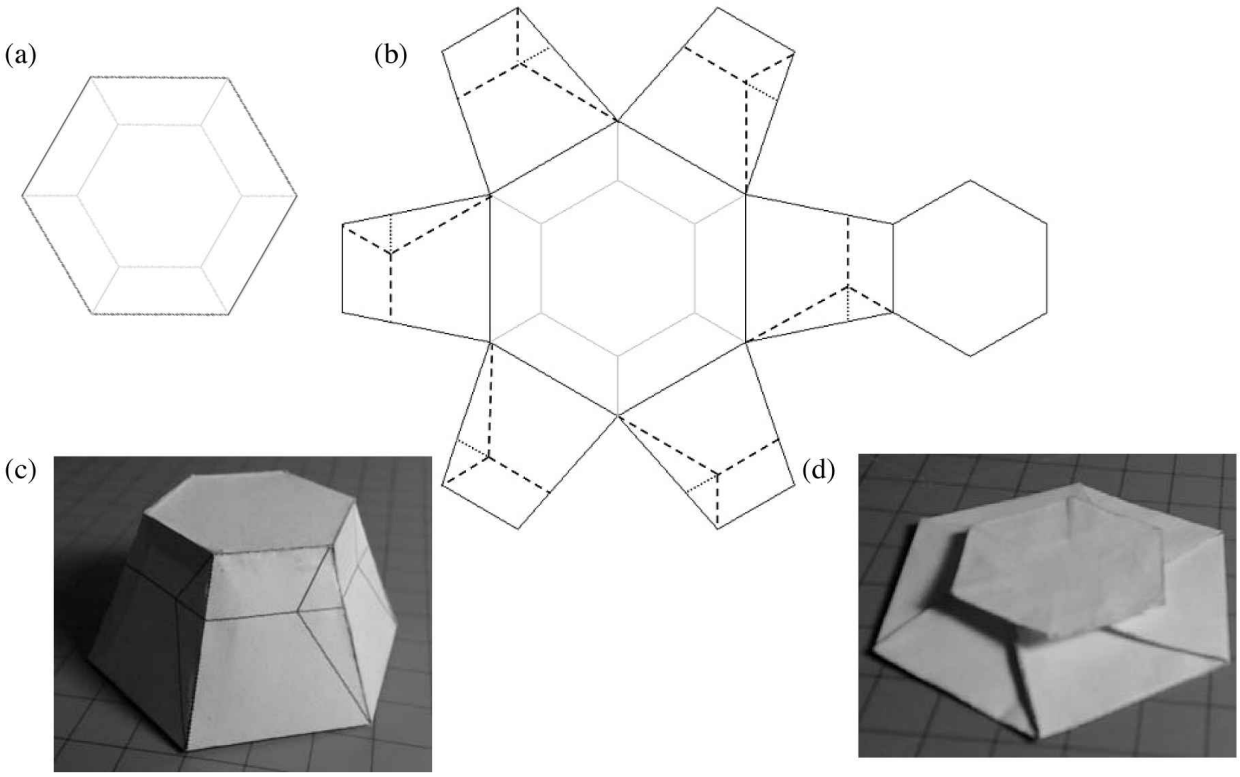

Fig 20: Example 1

Example 2 (Fig 21) is an oblique prism whose roof plane and base plane have the same layout.

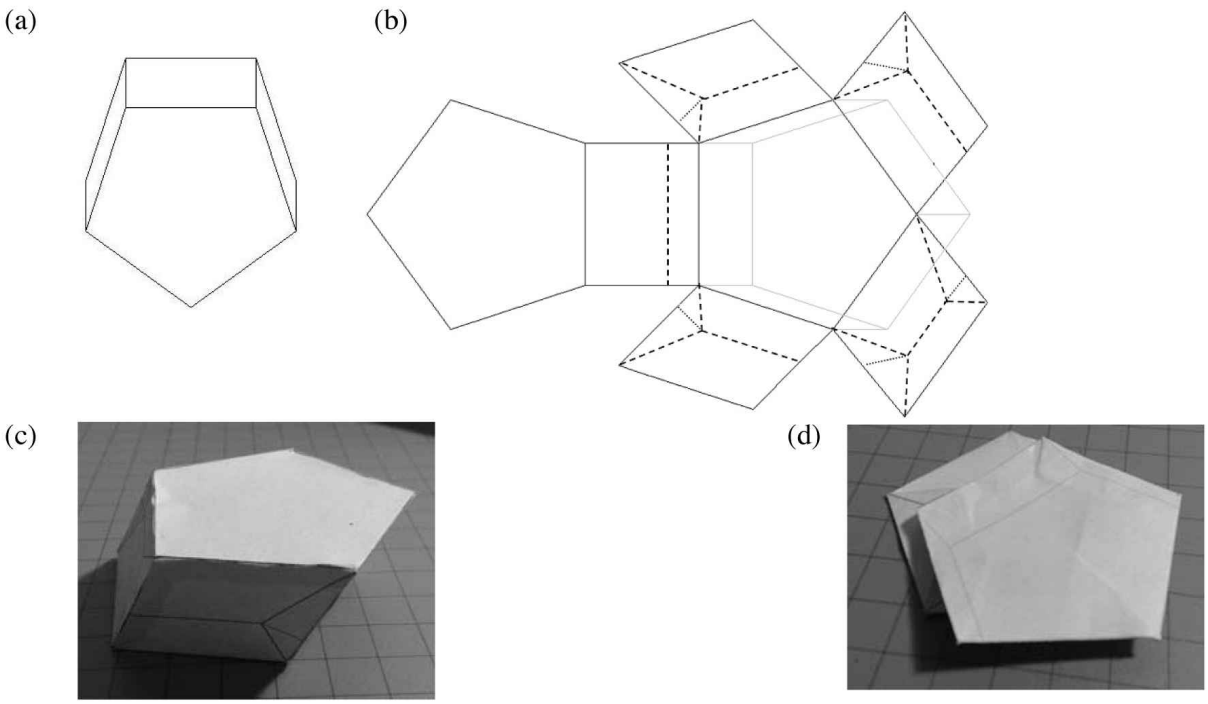

Fig 21: Example 2

Example 3 (Fig 22) is a cupola, whose base plane has twice vertices as many as its roof plane, and both planes are joined by alternating triangles and rectangles.

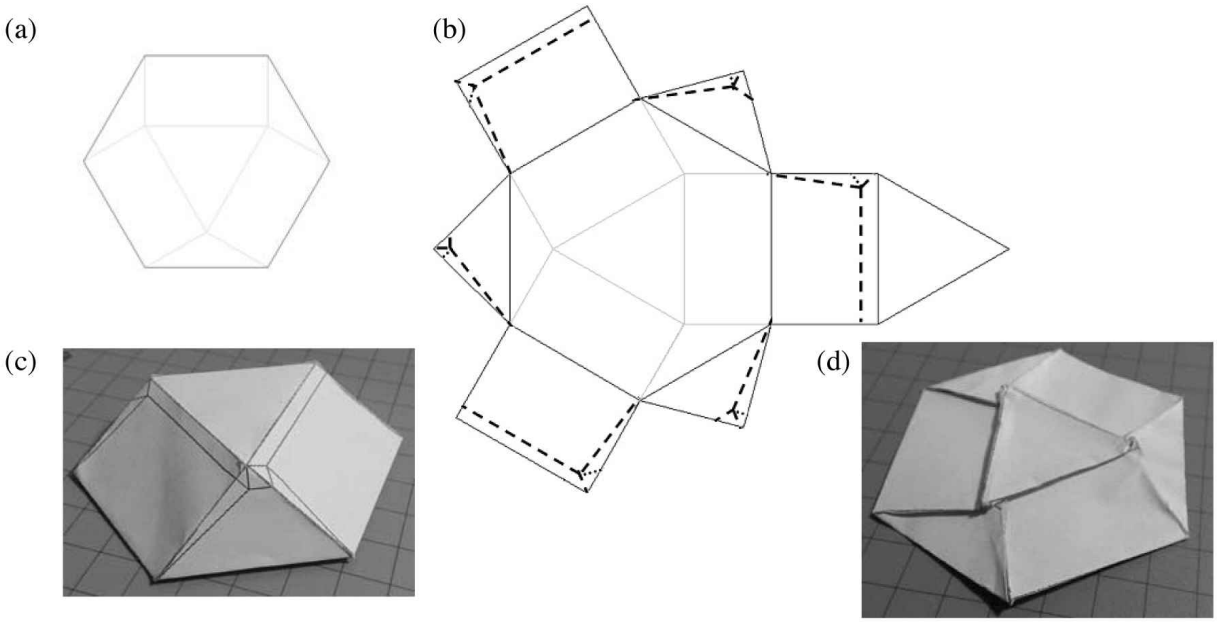

Fig 22: Example 3

Example 4 (Fig 23) is an antiprism which has only triangular lateral faces.

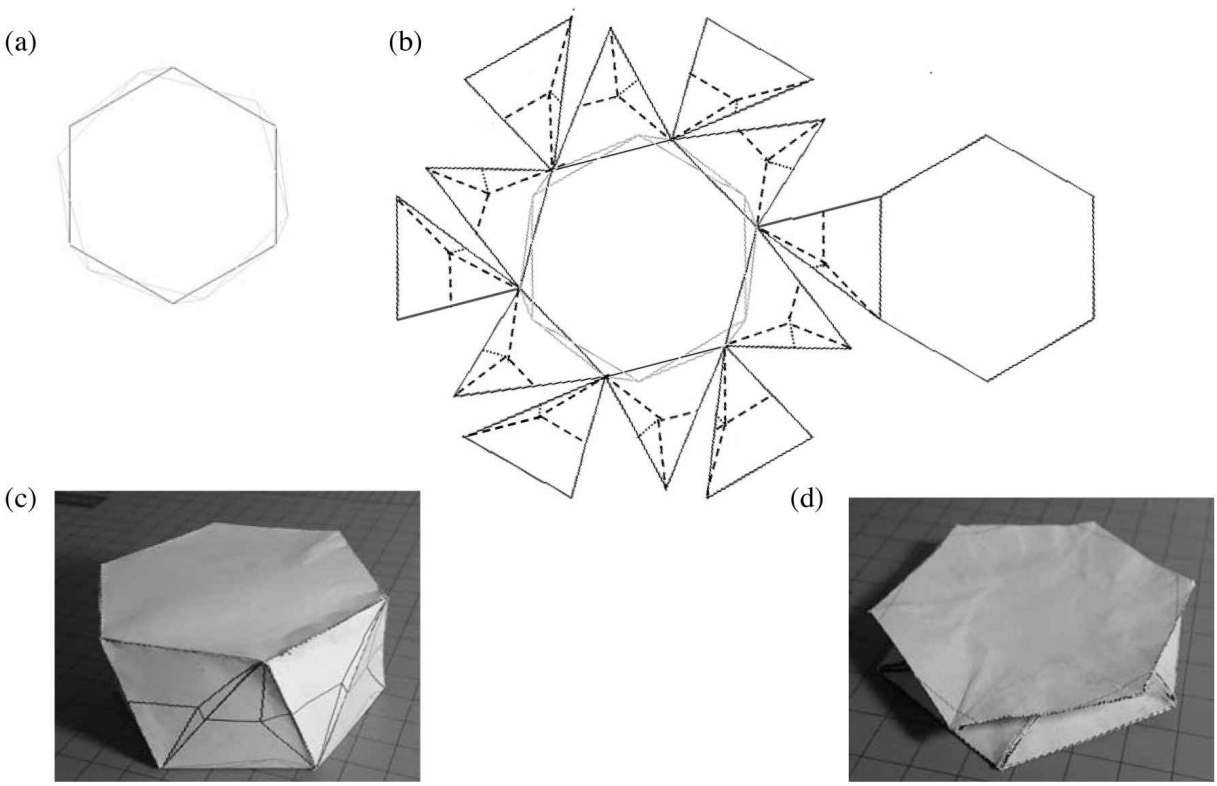

Fig 23: Example 4

Example 5 (Fig 24) is a convex prismatoid without any limitation.

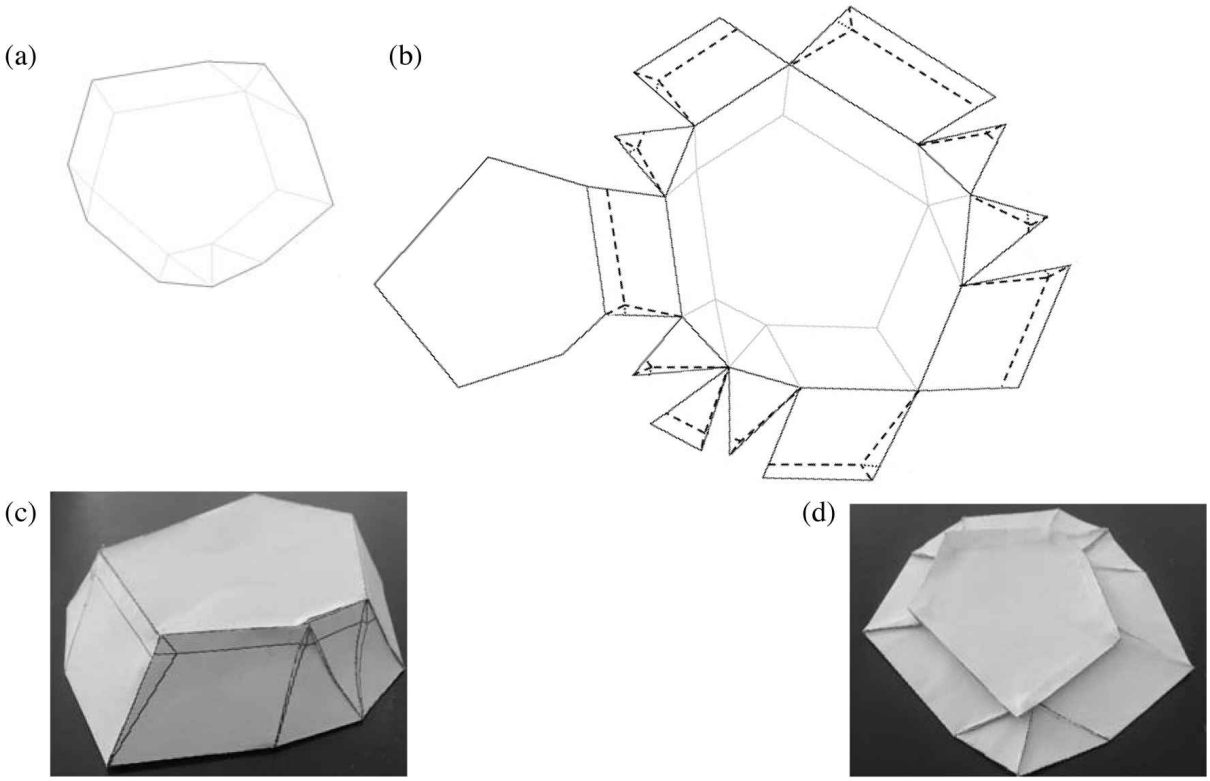

Fig 24: Example 5

Example 6 (Fig 25) is a convex prismatoid with limitation discussed in Theorem 7.

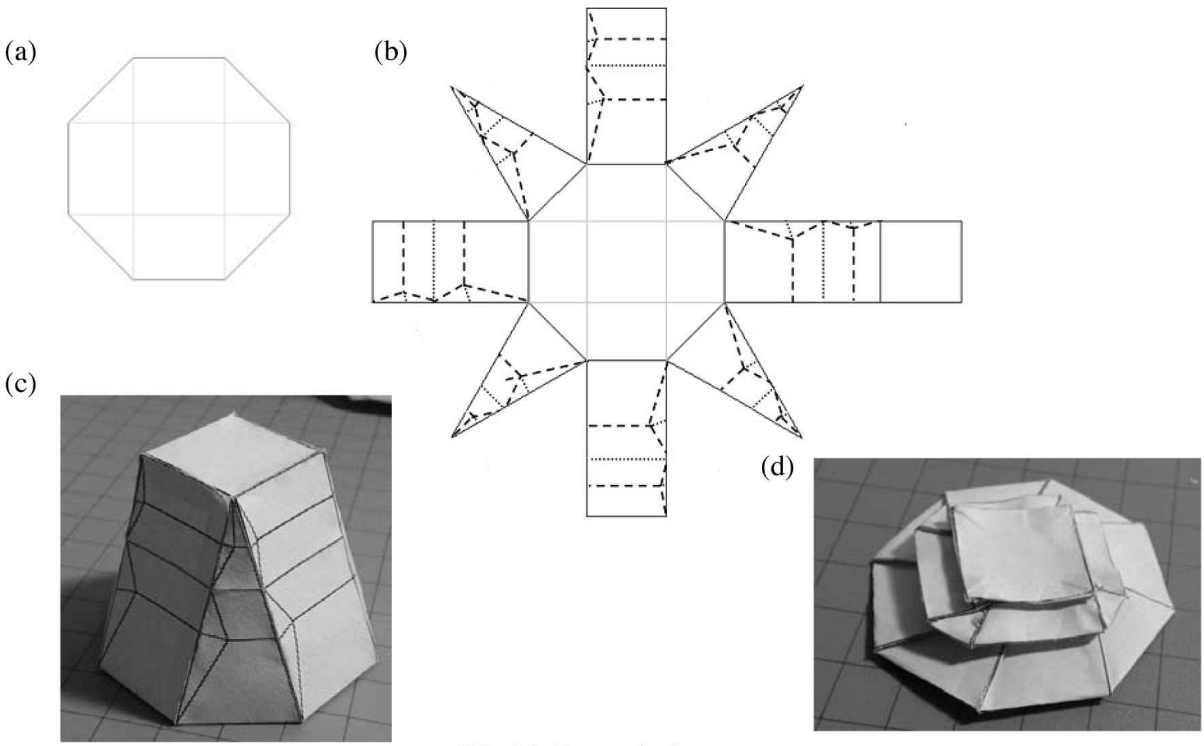

Fig 25: Example 6

Applications

Flattening of polyhedra has many applications in real life. In astronomy, scientists send space telescopes into outer space for observation of distant planets, galaxies, and other outer space objects. If one applies the method of flattening of polyhedron into rigid folding, it may help to reduce the space that the equipment takes up. These equipment can be restored to three-dimensional shape when there is a need to use them [4]. Our work is also applicable to robotics-making. Recently, George M. Whitesides' lab at Harvard has manufactured air-powered origami robotic actuators out of paper and elastic [5]. In the process of restoring the shape of flattened polyhedron, they make use of the force generated by air and lifted a weight which is over 100 times the weight of the actuator itself. Our work is also useful in biomedical appliances. Medical specialists may need trestles to temporarily hold a natural conduit open so that they can complete the operations successfully. In addition, our method can be applied to stents which are inserted into patients' bodies. The stents are flattened outside and expanded inside the organs to prevent or counteract a localized flow constriction [6].

Conclusion and discussion

In this paper, an original and novel method of flattening prismatoids has been proposed.
Each prismatoid is specified by its height and projection. All other lengths and angles of a prismatoid can be found by vector calculations once its height and projection are known.

The general algorithms are presented in the paper. By classifying the lateral faces (quadrilateral lateral face and triangular lateral face), one is able to draw valley line pattern on each lateral face by following the algorithms.

Limitation existed in Case I (quadrilateral lateral face) has been solved by dividing the whole prismatoid into several sections. The detailed method is presented in Theorem 7.
Although there are other methods besides the one presented here to flatten prismatoids, our method has clear advantages.

For example, one of the conventional methods is 'triangularization'. The intuition is by 'slicing' any prismatoid into several triangular pyramids and flattening each of them separately, as shown below.

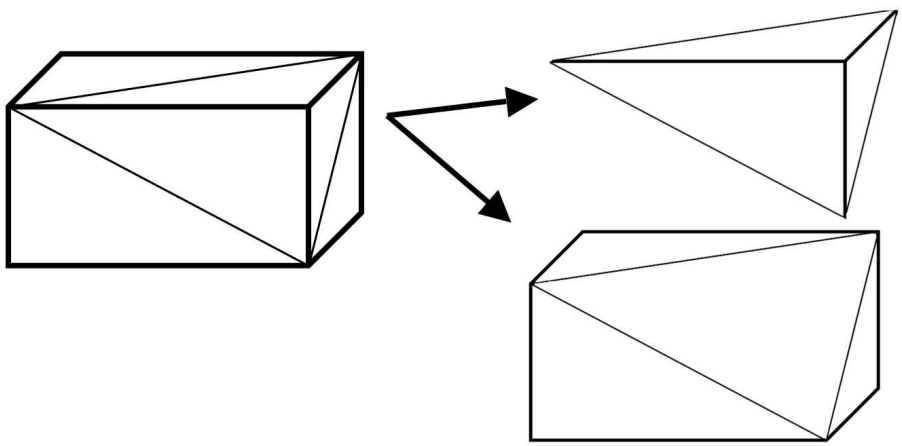

Fig 26: Triangularization

Our algorithm can handle much more complex geometry. Conventional method like triangularization is unable to do so because triangular pyramid does not exist all the time.

In terms of computation, since the resultant pattern using our 'Valley Line Method' is exactly the same as the projection of original prismatoid, one can more easily visualize the crease pattern. There is always a systematic way to compute the expended view of the prismatoid. However, conventional method needs to derive the 'new face', which is not trivial.

In terms of practicality, the conventional method (triangularization) runs into thickness issue very easily compared to our method. This means our algorithm can be applied to a wider range of real-life applications.

In future work, we will look into non-parallel planes and tackle with more complex geometries.

Acknowledgment

We would like to express our gratitude to our teacher-supervisor, Mr. Cheong Kang Hao, for all his efforts put in to improve our work in terms of writing and presentation. In the process, he supported us to face and overcome difficulties, which helps us to persevere until completing the project.

References

[1] E. D. Demaine, M. L. Demaine, *Recent Results in Computational Origami*, In Proceedings of the 3rd International Meeting of Origami Science, Math, and Education (OSME 2001), Monterey, California (2001), 3–16.

[2] E. D. Demaine, J. O'Rourke, *Geometric Folding Algorithms: Linkages, Origami, Polyhedra*, Cambridge University Press, New York, 2007.

[3] M. Bern, B. Hayes, *Origami Embedding of Piecewise-Linear Two-Manifolds*, Lecture Notes in Computer Science, **4957** (2008), 617-629.

[4] C. M. Chia, S. Debnath, *Origami and its Applications in Automotive Field*, 2nd International Conference, CUTSE, Sarawak, Malaysia (2009), 46-49.

[5] S&T News Bulletin, The latest in Science and Technology Research News, **2(7)**, 2012

[6] K. Kuribayashi, K. Tsuchiya, Z. You, D. Tomus, M. Umemoto, T. Ito, and M. Sasaki, *Self-Deployable Origami Stent Grafts as a Biomedical Application of Ni-rich TiNi Shape Memory Alloy Foil*, Mat. Sci. Eng. A-Struct., **419** (2006) 131–137.

The authors are students of NUS High School of Mathematics and Sciences.